

Application to nonlinear circular ring of nonlinear system identification based on AR time series analysis

Soichiro Takata^{1, a}

¹Department of Mechanical Engineering, National Institute of Technology, Tokyo College, 1220-2 Kunugida-machi, Hachioji-shi, 193-0997, Japan

^a<takata@tokyo-ct.ac.jp>

Keywords: cylindrical shell, nonlinear vibration, system identification, Kalman filter

Abstract. Previously, a method was proposed for identifying nonlinear parameters using Auto-Regressive time series analysis and the method of averaging; however, the application to the actual structure deterioration detection problem was not considered. Here, the method's application to a nonlinear circular ring is described, for use in the pipe thinning detection problem. First, the identification problem is formulated by applying the averaging method to Evensen's nonlinear circular ring model. The regression problem is formulated using the difference between the instantaneous natural angular frequency and the linear natural angular frequency. Operational validation of the proposed identification method is performed using numerical simulations based on the fourth order Runge-Kutta method. Furthermore, numerical analysis of the pipe thinning detection problem using the angular frequency and nonlinear coefficient is described.

1. Introduction

Many pipes for water, gas, and oil distribution experience deterioration owing to their prolonged utilization. Accidents caused by leaks and bursts result in service interruptions and supply disruptions. Appropriate maintenance is required for preventing accidents. Pipe renewal based on the results of non-destructive testing (NDT) is important for efficient maintenance.

NDT technology that detects a change in the pipe eigen frequency owing to the pipe thickness change has been proposed [1,2,3,4]. The method focuses on the in-plane bending vibration mode of a cylindrical shell [5,6,7]. The above NDT method is based on the eigenfrequency change of the in-plane bending mode of a cylindrical shell. Therefore, the sensitivity to the pipe thickness decreases based on the linear relationship between the eigenfrequency and the pipe thickness. Sensitivity improvement beyond that achieved using the previously proposed method is required for more effective maintenance operations.

Previously, an identification method was proposed based on the Auto-Regressive (AR) time series analysis using the data for transient free vibrations [8,9]. The proposed identification method was composed of a regression formula using the Krilov-Bogoliubov-Metropolsky (KBM) method, high-precision estimation of instantaneous frequency using a Kalman filter, and estimation of instantaneous amplitude using the Hilbert transform. An important advantage of the proposed method was its identification ability using a small number of samples. However, the application of the method to the actual deterioration detection was not considered [10]. In this study, the application to a nonlinear circular ring is described, for solving the pipe thinning detection problem.

First, the identification problem is formulated by applying the method of averaging to Evensen's nonlinear circular ring model [11]. The regression equation is obtained using the approximation solution of the amplitude-dependent eigenfrequency. Operational validation of the proposed identification method is performed using numerical simulations based on the Runge-Kutta method. Numerical analysis of the pipe thinning detection problem is conducted using the angular frequency and nonlinear coefficient.

2. Formulation of the identification problem

2.1 Analytical consideration based on the method of averaging

The model of a circular cylindrical ring is shown in Fig. 1. The coordinate axes are as follows: the axial coordinate is x , the polar coordinate is y , and the radial coordinate is z . The pipe width is b , the pipe radius is R , and the pipe thickness is h . In addition, the displacements of each coordinate are as follows: the deflection in the radial direction is w , and the displacement in the circumferential direction is v .

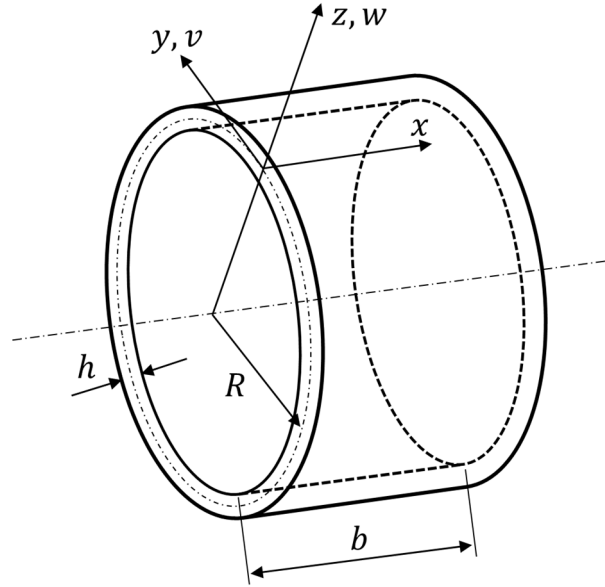


Fig. 1. Model of circular a cylindrical ring.

According to Evensen [11], the Lagrangian for the case of the in-extensional vibration (no stretching of the middle surface of the shell) is given by Eq. (1).

$$L = \frac{\rho h l}{2} \left(\frac{dA_n}{dt} \right)^2 \left\{ \pi R + \frac{n^4 A_n^2}{2R} \pi \right\} - \frac{E l h^3}{24(1 - \nu^2)} A_n^2 \left(\frac{n}{R} \right)^4 \pi R \quad (1)$$

Here, Young's modulus is E , pipe density is ρ , Poisson's ratio is ν , and wave number in circumferential direction is n . In addition, we assume the following deflection function:

$$w = A_n(t) \cos \frac{ny}{R} - \frac{1}{4} \frac{n^2}{R} A_n^2(t) \quad (2)$$

Here, $A_n(t)$ represents the modal coordinate of the n -th wave number. The non-dimensional equation of motion is obtained as follows using the non-dimensional coordinate $\zeta_n = A_n/h$ and the non-dimensional nonlinear parameter ϵ :

$$\frac{d^2 \zeta_n}{dt^2} + \frac{1}{2} \epsilon \zeta_n \left(\zeta_n \frac{d^2 \zeta_n}{dt^2} + \left(\frac{d\zeta_n}{dt} \right)^2 \right) + \zeta_n = 0. \quad (3)$$

Here, the linear eigenangular frequency ω_n and the non-dimensional nonlinear parameter ϵ are as follows:

$$\omega_n^2 = \frac{E}{\rho R^2} \frac{(n^2 - 1)^2}{12(1 - \nu^2)} \left(\frac{h}{R}\right)^4, \quad \epsilon = \frac{n^4 h^2}{R^2}. \quad (4)$$

The amplitude and phase equations are obtained from Eqns. (3) and (4) using the method of averaging. Here, a represents the amplitude, and φ represents the phase.

$$\frac{da}{dt} = 0 \quad (5)$$

$$\frac{d\varphi}{dt} = -\frac{\epsilon}{8} \omega_n a^2 / \left(1 + \frac{3\epsilon}{16} a^2\right) \quad (6)$$

The approximate solution of the eigenangular frequency is obtained by neglecting the high-order infinitesimal of ϵ .

$$\omega(a)^2 = \omega_n^2 \left(1 - \frac{\epsilon}{4} a^2\right) \quad (7)$$

2.2 Derivation of the nonlinear parameter regression formula

The formula for estimating the nonlinear stiffness parameter is obtained based on Eq. (7). The regression formula based on the least-squares method is given by Eqns. (8) ~ (10).

$$\begin{bmatrix} \omega(t_1)^2 \\ \vdots \\ \omega(t_N)^2 \end{bmatrix} = \begin{bmatrix} 1 & -a(t_1)^2/4 \\ \vdots & \vdots \\ 1 & -a(t_N)^2/4 \end{bmatrix} \begin{bmatrix} \alpha \\ \beta \end{bmatrix} \quad (8)$$

$$\mathbf{Y} = \begin{bmatrix} \omega(t_1)^2 \\ \vdots \\ \omega(t_N)^2 \end{bmatrix}, \mathbf{X} = \begin{bmatrix} 1 & -a(t_1)^2/4 \\ \vdots & \vdots \\ 1 & -a(t_N)^2/4 \end{bmatrix}, \boldsymbol{\theta} = \begin{bmatrix} \alpha \\ \beta \end{bmatrix} = \begin{bmatrix} \omega_n^2 \\ \epsilon \omega_n^2 \end{bmatrix} \quad (9)$$

$$\boldsymbol{\theta} = (\mathbf{X}^T \mathbf{X})^{-1} \mathbf{X}^T \mathbf{Y} \quad (10)$$

Where, t_1, \dots, t_N represent the discrete time.

3. Flowchart

A flowchart of the proposed identification method is shown in Fig. 2. The algorithm is composed of the instantaneous eigenangular frequency estimation and the amplitude estimation. The instantaneous eigenangular frequencies are inferred by estimating the time-varying AR model based on the parameter estimation problem of the Kalman filter. The instantaneous eigenangular frequencies are obtained from the characteristic root of AR coefficient polynomial. The instantaneous amplitude is calculated using the Hilbert transform. The nonlinear coefficients are estimated using the derived regression formula in the above section, using the instantaneous eigenangular frequency and the instantaneous amplitude.

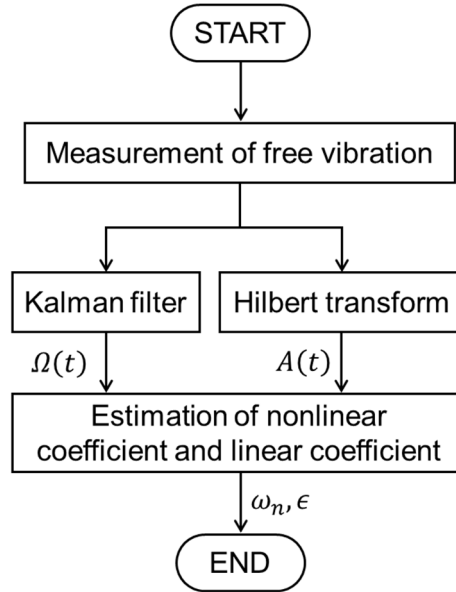


Fig.2. Flowchart of the proposed identification algorithm.

4. Verification of the fundamental operation

4.1 Conditions

The calculation conditions are presented in Table 1. Here, $dt = 0.10$ is the sampling time, $\zeta(0) = 5$ and $\dot{\zeta}(0) = 0$ are the initial conditions, the linear eigenangular frequency is $\omega_n = 1$, $\beta = 0.005$ is the damping ratio, and $\epsilon = 0.005$ is the nonlinear spring coefficient. The time dependence of the free oscillation is shown in Fig. 3, while the dependence of the restoring force on the displacement is shown in Fig. 4. Here, the restoring force means the amount of the linear spring force was divided the amplitude dependence mass. The restoring force was symmetric in the region between the tensile and compression sides.

Table 1 Values condition of nonlinear parameters and initial conditions

dt	ω_n	β	ϵ	$\zeta(0)$	$\dot{\zeta}(0)$
0.1	1.0	0.005	0.005	5.0	0.0

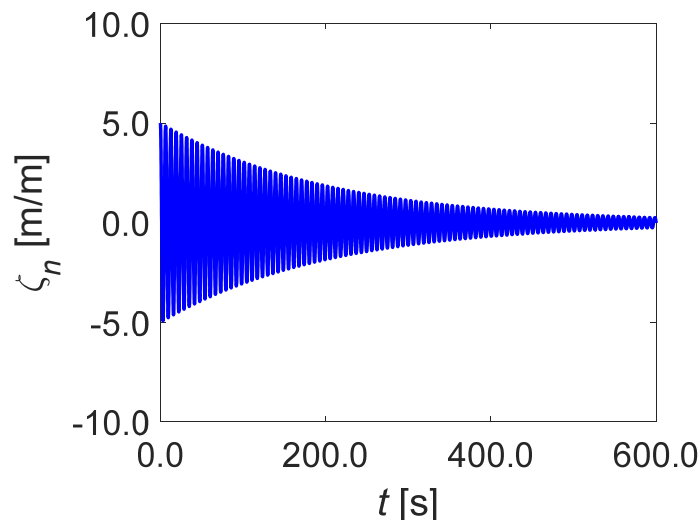


Fig.3. Time dependence of the nonlinear free vibration, for the modal coordinate.

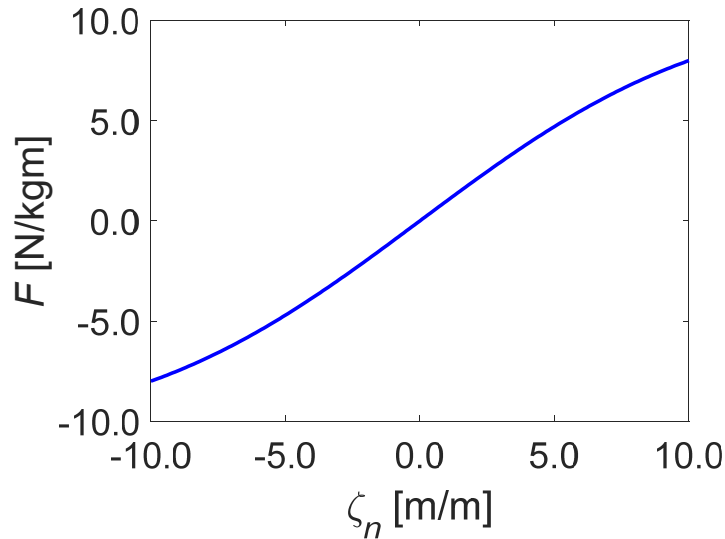


Fig.4. Restoring force vs. deformation.

4.2 Results and discussion

The estimation results of the instantaneous eigenangular frequency using the Kalman filter are shown in Fig. 5. Here, the vertical and horizontal axes represent the eigenangular frequencies and time, respectively. The calculation conditions were as follows: the time series model used the time-varying AR(M) model (here, $M = 8$), the covariance of the system noise is $\sigma_v^2 = 1$, the covariance of the observation noise was $\sigma_w^2 = 10^{-2}$, the initial value of the error covariance matrix was $P[0] = 10^6 \mathbf{I}$ (where, \mathbf{I} is the $M \times M$ identity matrix), and the initial value of the unknown AR coefficient vector was $\boldsymbol{\theta}[0] = \mathbf{0}$ (where, $\mathbf{0}$ is the $1 \times M$ zero vector). Here, the black dotted line represents the region of the time series that used the identification algorithm.

The estimated value of the instantaneous angular eigenfrequency gradually increased. Moreover, it converged to a constant value of the eigenangular frequency. The eigenangular frequency of the linear system was 1.00 rad/s, and the estimated converged eigenangular frequency was 0.9997 rad/s. Therefore, the estimated converged eigenangular frequency agreed well with the actual linear eigenangular frequency.

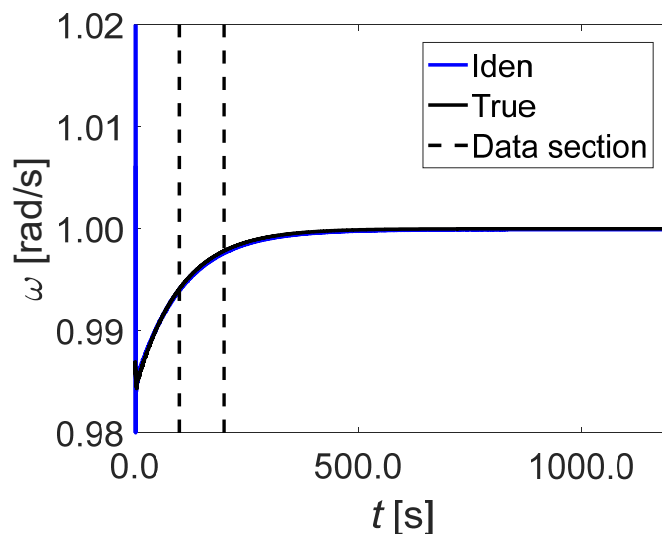


Fig.5. Estimated instantaneous angular frequency.

The estimation results of the relationship between the restoring force and displacement are shown in Fig. 6. Here, the vertical and horizontal axes represent the restoring force and the displacement, respectively. In addition, the black circle and blue solids curves show the true and estimated values, respectively. The estimated coefficients are listed in Table 2. The error rates of the linear eigenangular frequency and the non-dimensional nonlinear parameter were 0.03% and 2%, respectively. Hence, the operation of the proposed identification algorithm was confirmed. The estimated relationship between the restoring force and the displacement was identical to the actual one. In this method, the estimation accuracy of the parameter depends on the initial amplitude. Especially, the accuracy decreasing expects in case of the small initial amplitude.

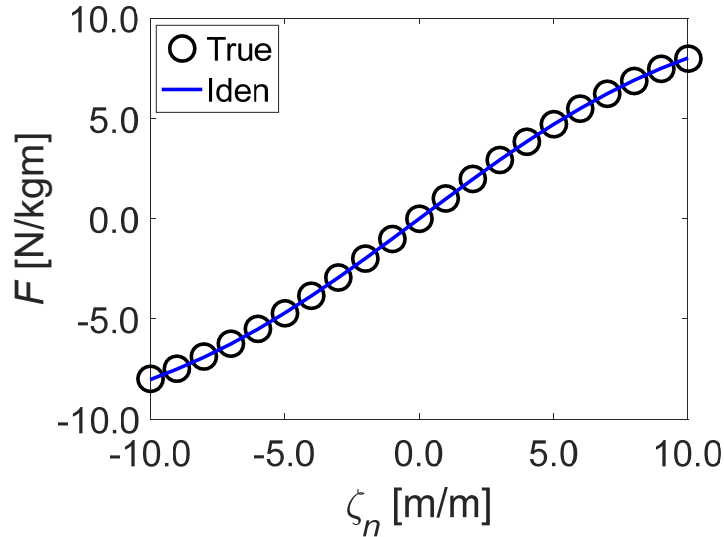


Fig.6. Estimated relationship between the restoring force and the displacement.

Table 2 Estimation results of the linear and nonlinear parameters.

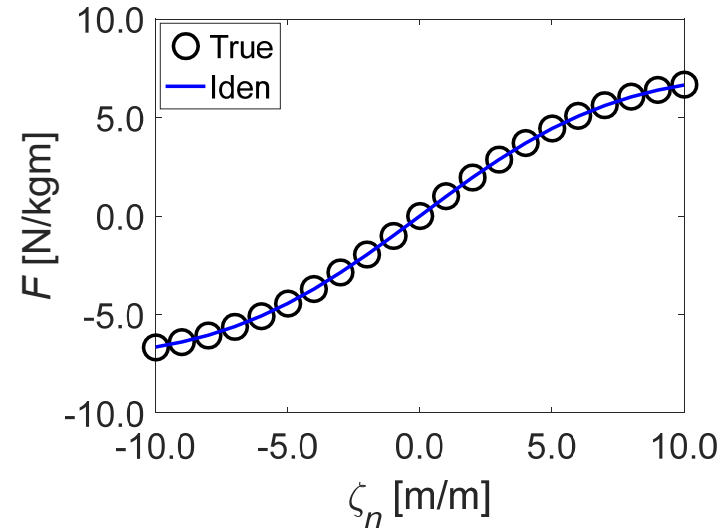
Values	ω_n	ϵ
True	1.0000	0.0050
Estimation	0.9997	0.0049

4.3 Performance dependence on the nonlinear coefficient

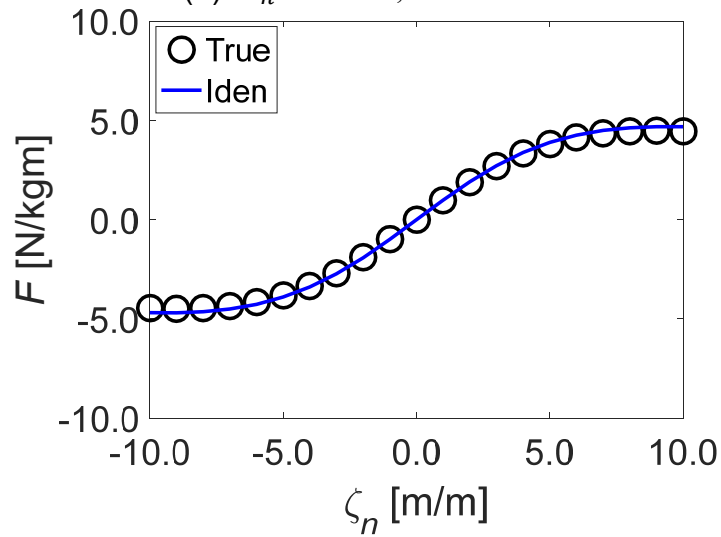
In this section, the dependence of the system identification method’s performance on the nonlinear parameter is considered. The calculation results for the relationship between the displacement and the restoring force are shown in Fig. 7. Here, panel (a) shows the results for $\omega_n = 1.000, \epsilon = 0.010$, panel (b) shows the results for $\omega_n = 1.000, \epsilon = 0.025$, and panel (c) shows the results for $\omega_n = 1.000, \epsilon = 0.050$. The estimated values are listed in Tabel 3.

Table 3 Estimation results of the linear and nonlinear parameters.

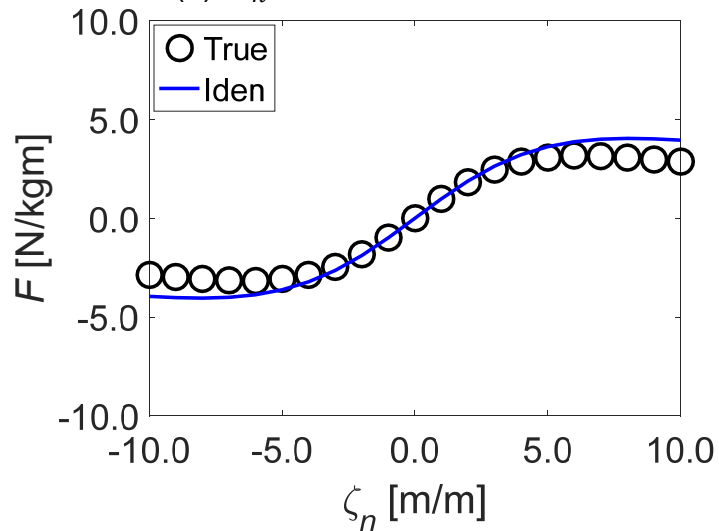
Condition	True	Estimation
(a)	$\omega_n = 1.000$	$\omega_n = 0.9998$
	$\epsilon = 0.010$	$\epsilon = 0.0097$
(b)	$\omega_n = 1.000$	$\omega_n = 0.9988$
	$\epsilon = 0.025$	$\epsilon = 0.0227$
(c)	$\omega_n = 1.000$	$\omega_n = 0.9894$
	$\epsilon = 0.050$	$\epsilon = 0.0382$



(a) $\omega_n = 1.000$, $\epsilon = 0.01$



(b) $\omega_n = 1.000$, $\epsilon = 0.025$



(c) $\omega_n = 1.000$, $\epsilon = 0.05$

Fig.7. Estimation results of the relationship between the restoring force and the displacement.

For case (a), the estimated value of the linear angular frequency was 0.9998 (compare to the true value of 1.000), and the estimated value of the nonlinear parameter was 0.0097 (compare to the true value of 0.010). For case (b), the estimated value of the linear angular frequency was 0.9988 (compare to the true value of 1.000), and the estimated value of the nonlinear parameter was 0.0227 (compare to the true value of 0.0250). For case (c), the estimated value of the linear angular frequency was 0.9894 (compare to the true value of 1.000), and the estimated value of the nonlinear parameter was 0.0382 (compare to the true value 0.0500). In each case, the estimated values of the linear angular frequency and the nonlinear parameter agreed well with the true values.

6. Numerical analysis of the pipe thinning detection problem

In this section, the numerical analysis of the pipe thinning detection problem is presented. Here, the test pipe was assumed to be a thin aluminum ring [12], and the following numerical conditions were assumed: Young’s modulus $E = 68$ GPa, density $\rho = 2800$ kg/m³, Poisson’s ratio $\nu = 0.3$, thickness $h = 0.05 - 0.11$ mm, and radius $R = 32.5$ mm. The thickness dependence of the estimated values is shown in Fig. 8. Here, the horizontal axis represents the pipe thickness, the left vertical axis shows the angular frequency, and the right vertical axis shows the nonlinear coefficient. In addition, the black circles show the estimated angular frequency, the blue circles show the estimated nonlinear coefficient, the black solid line shows the true angular frequency, and the blue solid line shows the true nonlinear coefficient. The estimated values agree well with the corresponding true values, in all cases.

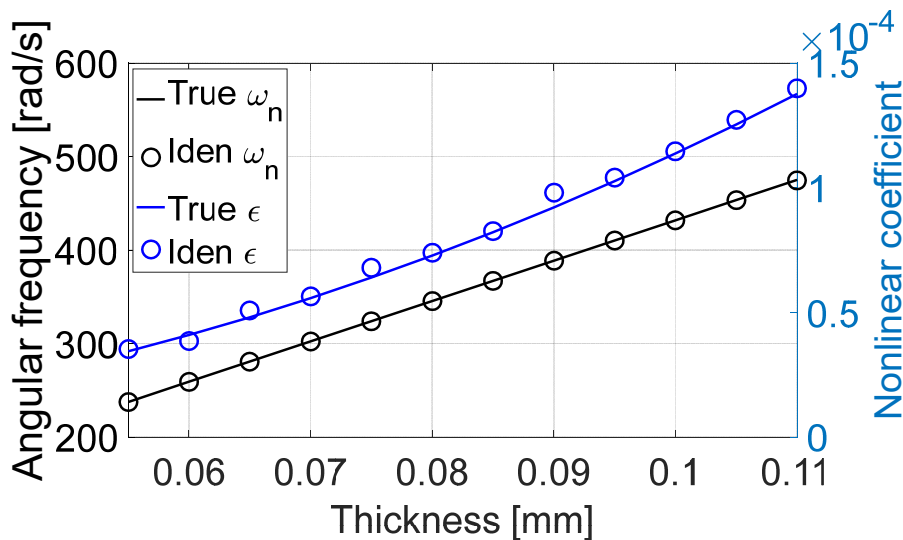


Fig. 8. Thickness dependence of estimated values.

A linear change in the estimated value with respect to the pipe thickness thinning was observed in the case of the angular frequency. On the other hand, a nonlinear change in the estimated value with respect to the pipe thickness thinning was observed in the case of the nonlinear coefficient. Here, the sensitivity of the pipe thinning was defined by the thickness derivative with respect to the ratio between the estimated value and the nominal value. In the thinning process with a nominal thickness of 0.11 mm to a thinning thickness of 0.10 mm, the ratio of the eigen-angular frequency decreased by 0.09%. In addition, the sensitivity of the eigen-angular frequency with respects to the pipe thinning did not depend on the pipe thickness. On the other hand, in the case of the above thinning process, the ratio of the nonlinear coefficient decreased by 0.1798%. Therefore, the sensitivity of the pipe thinning detection in the case of the nonlinear coefficient was higher than that in angular frequency case.

In general, the sensitivity of the pipe thinning detection using the nonlinear coefficient depends on the pipe thickness. Theoretically, the sensitivity of the nonlinear coefficient is higher than that of the angular frequency when the pipe thickness is over half. Therefore, under this calculation condition, a high sensitivity for the initial pipe thinning detection (i.e., deterioration sign) is implied.

7. Conclusion

In this study, we considered the application of a nonlinear stiffness identification method based on the AR time-series analysis to a nonlinear circular ring. Consequently, the following results were obtained.

(1) The identification algorithm for a nonlinear circular ring was derived based on the averaging method.

(2) Operation validation using the numerical experiment was conducted using the fourth order Runge-Kutta method, and the estimated values of the eigenangular frequency and the nonlinear coefficient agreed well with the corresponding true values.

(3) A numerical analysis of the pipe thinning detection problem was conducted. As a result, the sensitivity for the pipe thinning detection in the case of the nonlinear coefficient was higher than that in the angular frequency case. The high sensitivity for the pipe thinning detection in the early stage is suggested.

Acknowledgments

This work was supported by JSPS KAKENHI Grant Number JP20K14685.

References

- [1] H. Inoue, S. Takata and S. Shinoda, "Simplified description of in-plane bending mode of cylindrical shell using two-dimensional ring model", *Symposium on Evaluation and Diagnosis 16*, 109, 2017 (in Japanese).
- [2] S. Shinoda, H. Inoue and S. Takata, "Thinning pipe wall detection using coupled oscillation between cylindrical shell and attached sub-structure", *Symposium on Evaluation and Diagnosis 16*, 104, 2017 (in Japanese).
- [3] S. Takata, H. Inoue and S. Shinoda, "Vibration analysis of cylindrical shell with sub-structure using Semi-Analytical Receptance Method", *Symposium on Evaluation and Diagnosis 16*, 108, 2017 (in Japanese).
- [4] S. Takata, H. Inoue and S. Shinoda, "Proposal of the pipe diagnosis method using in-plane bending vibration of cylindrical shell", *Transactions of the Japan Society of Mechanical Engineers*, Vol.84, No.861, DOI:10.1299/transjsme.17-00522, 2018 (in Japanese).
- [5] J. P. Den Hartog, "Mechanical vibrations", *Dover Publications*, p.165-p.169, 1985.
- [6] W. Flugge, "Statik and dynamic der schalen 3rd ed", *Springer*, 1962.
- [7] A. H. E. Love, "The mathematical theory of elasticity 4th ed", *Macmillan*, 1959.
- [8] S. Takata, S. Kinoshita, T. Kumura and Y. Sasaki, "Nonlinear mechanical system identification method using auto-regression time series analysis", *Transactions of the Japan Society of Mechanical Engineers*, Vol.81, No.824, DOI:10.1299/transjsme.14-00564, 2015 (in Japanese).
- [9] S. Takata, "Identification of nonlinear spring coefficient in asymmetric nonlinear system using auto-regressive time series analysis", *Transactions of the Japan Society of Mechanical Engineers*, Vol.86, No.881, DOI:10.1299/transjsme.19-00172, 2019 (in Japanese).

Journal of Mechanical and Electrical Intelligent System (JMEIS)

- [10] S. Takata, M. Habashi and S. Tarao, "Nonlinear stiffness identification based on AR time series analysis using transient free oscillation", *Journal of Mechanical and Electrical Intelligent System*, Vol.4, No.1, pp.26–35, 2021.
- [11] D. A. Evensen, "A theoretical and experimental study of the nonlinear flexural vibrations of thin circular rings", *NASA Technical Report*, NASA TR R-227, 1965.
- [12] T. Ito and S. Takata, "Vibration analysis of in-plane bending mode in coupled cylindrical shell using coupled circular ring model for pipe thickness estimation", *Journal of Mechanical and Electrical Intelligent System*, Vol.4, No.3, pp.23–33, 2021.